

Numerical Simulations of Two-dimensional Electron Fluid: An Application of Classical-map Hypernetted-chain Method

Chieko TOTSUJI, Takashi MIYAKE, Kenta NAKANISHI,
Kenji TSURUTA, and Hiroo TOTSUJI
Graduate School of Natural Science and Technology and Faculty of Engineering,
Okayama University, Tsushimanaka 3-1-1,
Okayama 700-8530, Japan

(Received December 12, 2007)

Based on the mapping introduced by the classical-map hypernetted-chain (CHNC) method, classical numerical simulations, Monte Carlo and molecular dynamics, have been applied to the two-dimensional electron fluid and the results are compared with those of quantum Monte Carlo simulations hitherto reported. It is shown that polarization properties of the ground state obtained by the diffusion Monte Carlo method are reproduced within the accuracy of quantum simulations by both of two mapping functions for the quantum temperature which have been proposed within the CHNC method. These results may serve as the basis of numerical simulations based on the CHNC method which are applicable to finite non-periodic systems like quantum dots and systems at finite temperatures.

I. INTRODUCTION

Properties of electron systems in three or two dimensions are of basic importance in designing various materials as electronic devices. In spite of a long history of their investigations, we still lack simple and, at the same time, accurate methods applicable to these quantum systems. With the development of mesoscopic manufacturing especially in two dimensions, there seems to exist an enhanced requirement for theoretical framework to handle two-dimensional electron systems of mesoscopic scale. We here analyze the validity of a method which is based on a mapping to classical system and easily applicable to finite systems and systems at finite temperatures.

We consider a system of electrons with the surface number density n at the temperature T and denote the spin components by suffices or superscripts $\sigma = \pm 1$ as

$$n = \sum_{\sigma} n_{\sigma}. \quad (1)$$

Our system is characterized by three parameters, the

r_s parameter defined by

$$r_s = (\pi n)^{-1/2}, \quad (2)$$

the spin polarization ζ defined by

$$\zeta = \frac{n_+ - n_-}{n_+ + n_-} = \frac{n_+ - n_-}{n}, \quad (3)$$

and T/T_F . We use the atomic units and take $k_B = 1$ in most of expressions.

Dharma-wardana and Perrot have developed the classical-map hypernetted-chain (CHNC) method[1] so as to reproduce the results of first principle quantum simulations for uniform interacting electron fluid by mapping the quantum system to the classical system. They assume that a quantum system at temperature T is mapped onto the classical fluid at the temperature T_{cf} given by

$$T_{cf} = (T_q^2 + T^2)^{1/2}. \quad (4)$$

Here T_q is the "quantum temperature" which expresses the effect of degeneracy in terms of a contribution to the temperature of classical fluid. They have given T_q as a function of r_s to reproduce the quantum

This work is subjected to copyright.
All rights are reserved by this author/authors.

pair distribution function in the ground state obtained by quantum Monte Carlo simulations. This method has been applied to infinite electron fluids in two or three dimensions and a variety of physical properties have been analyzed in the ground state and also at finite temperatures with arbitrary spin polarization[2–5].

The CHNC analyses by Dharma-wardana and Perrot have been made on the uniform unbounded systems through the integral equations which are simplified due to the translational invariance. For systems without the latter invariance or those with complicated geometry, however, it is not straightforward to apply the integral equations. Typical examples of those without translational invariance are quantum dots or multi-layered electron systems.

We here apply a method of numerical simulation based on the CHNC method to the two-dimensional uniform electron fluid and report the results. Our purpose is to confirm the applicability to systems with the translational invariance and establish a basis for applications to systems without it: Though integral equations are not simplified without the latter invariance, we can perform numerical simulations for those systems with exactly the same manner.

II. OUTLINE OF CLASSICAL-MAP HYPERNETTED-CHAIN METHOD

The CHNC method is composed of three elements: (a) The assignment of the temperature to include the effect of degeneracy, (b) the addition of a repulsive potential (the Pauli potential) between electrons with the same spin component to simulate the effect of Fermi statistics, and (c) the modification of the Coulomb potential to include the effect of diffraction.

For the system of electrons at the temperature T , the temperature of the corresponding classical fluid T_{cf} is assumed to be[1]

$$T_{cf} = \sqrt{T_q^2 + T^2}, \quad (5)$$

where the quantum temperature T_q expresses the effect of degeneracy. For three-dimensional electron fluids, T_q is expressed as

$$T_q/T_F = 1/(a + b r_s^{1/2} + c r_s) \quad (6)$$

with $a = 1.594$, $b = -0.3160$, $c = 0.0240$ and $r_s = (4\pi n/3)^{-1/3}$, n being the electron density[1]. Here T_F is defined by

$$k_B T_F = \sum_{\sigma=\pm 1} \frac{n_\sigma}{n} E_F^\sigma \quad (7)$$

and E_F^σ is the Fermi energy of spin species σ .

For two-dimensional electron fluids, the relation (TqI)

$$T_q/T_F = 2/[1 + 0.86413(r_s^{1/6} - 1)^2] \quad (8)$$

has been proposed[2]. This is based on a comparison of the values of the correlation energy E_c of fully polarized system with those obtained by Tanatar and Ceperley through the diffusion Monte Carlo (DMC) method[7]. Bulutay and Tanatar have proposed another expression (TqII)[3]

$$T_q/T_F = \frac{1 + a r_s}{b + c r_s} \quad (9)$$

with $a = 1.470342$, $b = 6.099404$, $c = 0.476465$ by fitting the correlation energy E_c to the expression proposed by Rapisarda and Senatore[6] obtained by DMC over the range $0.25 < r_s < 40$. In our analysis, we compare the results of numerical simulations obtained by adopting TqI and those obtained by adopting TqII.

The Pauli potential between electrons with the same spin species is determined so as to reproduce the exact correlation in the ideal Fermi gas within the hypernetted chain approximation. In a classical fluid at the temperature T_{cf} , the pair distribution function between particles of species σ and σ' is generally written as

$$g_{\sigma\sigma'}(r) = \exp[-\beta \phi_{\sigma\sigma'}(r) + h_{\sigma\sigma'}(r) - c_{\sigma\sigma'}(r) + B_{\sigma\sigma'}(r)], \quad (10)$$

where $\beta = 1/(k_B T_{cf})$, $\phi_{\sigma\sigma'}(r)$ is the pair potential, $h_{\sigma\sigma'}(r) = g_{\sigma\sigma'}(r) - 1$ is the pair correlation function, $c_{\sigma\sigma'}(r)$ is the direct correlation function, and $B_{\sigma\sigma'}(r)$ is the bridge function, respectively. Since the last function is neglected in the hypernetted chain approximation, the Pauli potential $P_{\sigma\sigma'} = \delta_{\sigma\sigma'} P_{\sigma\sigma}$ is determined from the pair correlation function in the ideal Fermi gas $h_{\sigma\sigma}^0 = \delta_{\sigma\sigma'} h_{\sigma\sigma}^0$ as

$$\beta P_{\sigma\sigma}(r) = -\ln(h_{\sigma\sigma}^0(r) + 1) + h_{\sigma\sigma}^0(r) - c_{\sigma\sigma}^0(r), \quad (11)$$

where the direct correlation function $c_{\sigma\sigma}^0(r)$ is given by the Ornstein-Zernike relation which is reduced to

$$h_{\sigma\sigma}^0(r) = c_{\sigma\sigma}^0(r) + n_\sigma \int d\mathbf{r}' h_{\sigma\sigma}^0(|\mathbf{r} - \mathbf{r}'|) c_{\sigma\sigma}^0(r'). \quad (12)$$

In the case of $T = 0$ considered in this paper, the correlation function in the ideal gas in two dimensions is given by

$$h_{\sigma\sigma}^0(r) = -\left(\frac{2J_1(k_F^\sigma r)}{k_F^\sigma r}\right)^2, \quad (13)$$

where $k_F^\sigma = 2(\pi n_\sigma)^{1/2}$.

The pair potential is given by

$$\phi_{\sigma\sigma'}(r) = P_{\sigma\sigma}\delta_{\sigma\sigma'} + V^{Coul}(r), \quad (14)$$

where the second term $V^{Coul}(r)$ is the Coulomb potential between electrons which is modified in order to take the effect of diffraction into account in two dimension as[2]

$$V^{Coul}(r) = \frac{1}{r}[1 - \exp(-k_{th}r)] \quad (15)$$

and

$$k_{th} = k_{th}^0 \times 1.158 (T_{cf})^{0.103}. \quad (16)$$

Here $k_{th}^0 = (2\pi m^* T_{cf})^{1/2}$ and $m^* = 1/2$ is the reduced mass of the scattering electron pair.

The total Helmholtz free energy of the system is divided into the ideal gas part F_{id} and the exchange-correlation part F_{xc} as

$$F = F_{id} + F_{xc}. \quad (17)$$

The the ideal gas part at $T = 0$ is given by

$$F_{id} = \sum_{\sigma} F_{id}^{\sigma} = n \sum_{\sigma=\pm 1} \frac{1}{4r_s^2} (1 + \sigma\zeta)^2. \quad (18)$$

The expectation value of the interaction part of the Hamiltonian, ε_{int} , is given by the pair correlation functions as

$$\varepsilon_{int} = \frac{n}{2} \int d\mathbf{r} \frac{e^2}{r} [\bar{g}(r) - 1] \quad (19)$$

where

$$\bar{g}(r) = \sum_{\sigma\tau} \frac{n_{\sigma}}{n} \frac{n_{\tau}}{n} g_{\sigma\tau}(r) \quad (20)$$

and the exchange-correlation part is obtained by an integration with respect to the scaled Coulomb coupling as

$$F_{xc}(r_s, \zeta) = n \int_0^1 \frac{d\lambda}{\lambda} \varepsilon_{int}(\lambda e^2, \zeta). \quad (21)$$

Here $\varepsilon_{int}(\lambda e^2, \zeta)$ is the expectation value of the interaction part of the Hamiltonian for the Coulomb coupling λe^2 .

III. NUMERICAL SIMULATION

We have performed numerical simulations of the classical system obtained by the mapping of the

CHNC method. The Hamiltonian of our system with N electrons is written as

$$\mathcal{H} = \sum_i^N \frac{\mathbf{p}_i^2}{2m} + \sum_{i>j}^N \frac{1 - \exp(-k_{th}r_{ij})}{r_{ij}} + \sum_{i>j}^N \delta_{\sigma_i\sigma_j} P_{\sigma_i\sigma_j}(r_{ij}), \quad (22)$$

where \mathbf{r}_i and σ_i are the position and spin of the particle i and $\mathbf{r}_{ij} = \mathbf{r}_i - \mathbf{r}_j$. The first term is the kinetic energy, the second term is Coulomb interactions with the effect of thermal diffraction, and the last term describes the Pauli potential between electrons with parallel spin.

In the case of two dimensions, it is shown that the asymptotic value of the Pauli potential for $r \rightarrow \infty$ is given by

$$\beta P(k_F^{\sigma}r) \sim \frac{\pi}{k_F^{\sigma}r}. \quad (23)$$

In our simulations, we have applied an interpolation formula for the Pauli potential

$$\beta P(k_F^{\sigma}r) = \frac{\pi}{k_F^{\sigma}r} \left[1 - \exp\{-1.95(k_F^{\sigma}r)^{0.85}\} \cos(1.5k_F^{\sigma}r) \right]. \quad (24)$$

This satisfies the asymptotic behavior and reproduces the values of Pauli potentials with the relative error less than 1% except for the region around $k_F^{\sigma}r = 2$, $1.5 < k_F^{\sigma}r < 2.5$ where the error is about 5%. We have confirmed these errors do not influence our results given in the next section by changing fitting parameters.

Molecular dynamics and the Monte Carlo simulations have been performed being imposed the periodic boundary conditions. The Ewald method has been used to evaluate the forces caused by Coulomb and the asymptotic part of the Pauli potential. For each combination of the parameters r_s and ζ , the system is relaxed to thermal equilibrium by the molecular dynamics and then the Monte Carlo method based on the Metropolis algorithm is applied. The numerical data have been obtained from the last part by the long enough Monte Carlo steps which allow exact control of the temperature. Examples of the size dependence in the calculation of Coulomb energy per electron in the system are shown in Table I. Based on these results, we have adopted $N = 256$.

The values of ε_{int} are computed from the pair distribution functions and interpolated in order to facilitate the integration with respect to the scaled coupling parameter Eq.(21) to obtain F_{xc} . Seven points in $2 \leq r_s \leq 40$ have been used for the interpolation by a power law with respect to r_s . The relative error of the interpolation is less than 1% for $15 \leq r_s$, from

TABLE I: The size dependence of the Coulomb energy for systems of $N = 256$ and $N = 512$ using function in Ref.[3].

	$N = 256$	$N = 512$
$r_s = 40, \zeta = 0$	-0.025739	-0.025739
$r_s = 40, \zeta = 1$	-0.025502	-0.025509
$r_s = 20, \zeta = 0$	-0.049929	-0.049941
$r_s = 20, \zeta = 1$	-0.049741	-0.049735

1% to 5% for the $2 \leq r_s \leq 15$, and more than 5% for $r_s \leq 1$. The errors for $\zeta = 0$ are slightly larger than those for $\zeta = 1$. The above errors are sufficiently small in order to derive the results in the next section.

IV. RESULTS AND DISCUSSIONS

We have adopted two mapping functions for T_q , Eq.(6) by Perrot and Dharma-wardana[2] denoted as function I hereafter, and Eq.(8) by Bulutay and Tanatar[3] denoted as function II. Some examples of pair distribution function are shown in Fig.1. We have

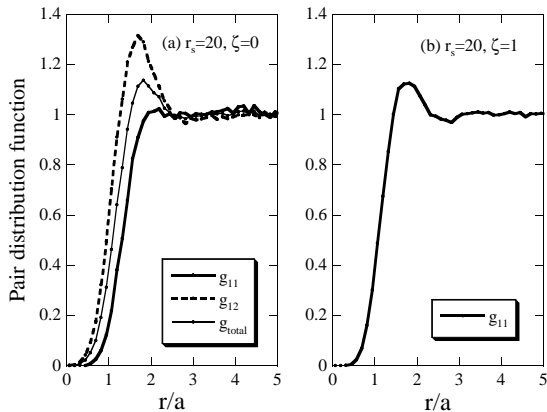


FIG. 1: Pair distribution functions by numerical simulation with mapping function I. (a) $r_s = 20$ and $\zeta = 0$, (b) $r_s = 10, 20, 40$ and $\zeta = 1$.

found that the first peaks of pair distribution function are always slightly lower and the first valley depths are a little less than those of DMC results. This is consistent with the results of CHNC analyses by integral equations, Fig.2 of Ref.[2] and Fig.3 of Ref.[3], though the reason is not clarified yet.

The results of Helmholtz free energy in atomic unit are shown in Figs.2 and 3 for mapping functions I and II, respectively. For given values of r_s and ζ , the energy in Fig.2 is always higher than that in Fig.3 and unpolarized system with $\zeta = 0$ is the ground state in

the region where r_s is less than 5 in both results.

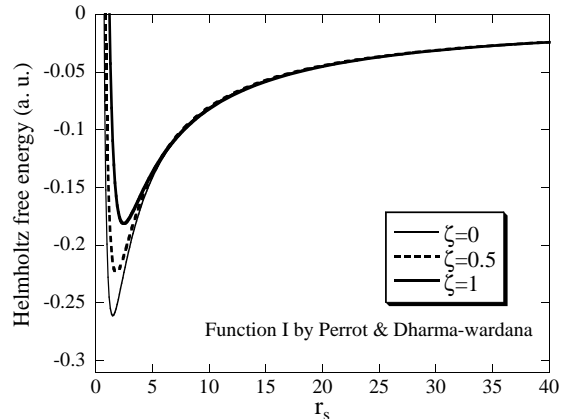


FIG. 2: Helmholtz free energy by numerical simulation with mapping function I.

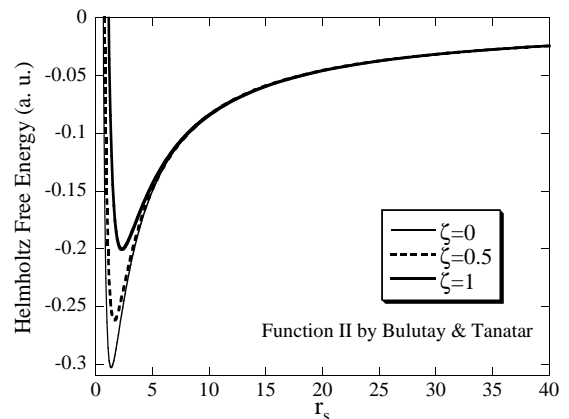


FIG. 3: Helmholtz free state energy by numerical simulation with mapping function II.

In order to observe the ground state polarization in detail, the excess of energies of $\zeta = 0.5$ and $\zeta = 1$ over $\zeta = 0$ are shown in Figs.4 and 5 for each mapping function. In Fig.4 we see that the ground state is polarized for the system with $8 \leq r_s \leq 38$ for mapping function I, and the energy of system with $\zeta = 0.5$ is always higher than systems with $\zeta = 0$. In case of mapping function II, the ground state is polarized for the system with $10 \leq r_s \leq 31$ as shown in Fig.5.

Some values of the ground state energy of the 2D electron fluid obtained are summarized in Table II and the values in references are given in Table III. The lowest energy values are denoted in italics in Table II. The differences between the results with two T_q mapping functions are less than a few % except for small r_s region and polarization properties are almost

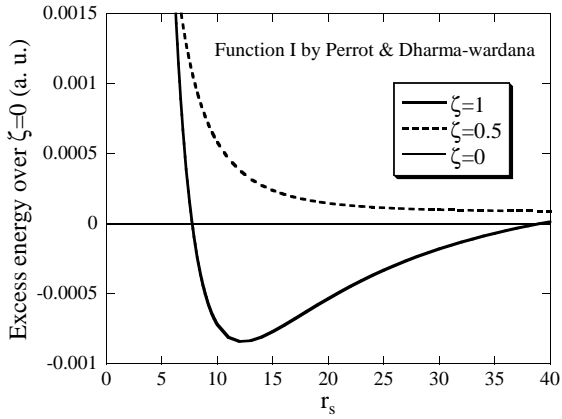


FIG. 4: Energy difference between polarizations by numerical simulation with mapping function I.

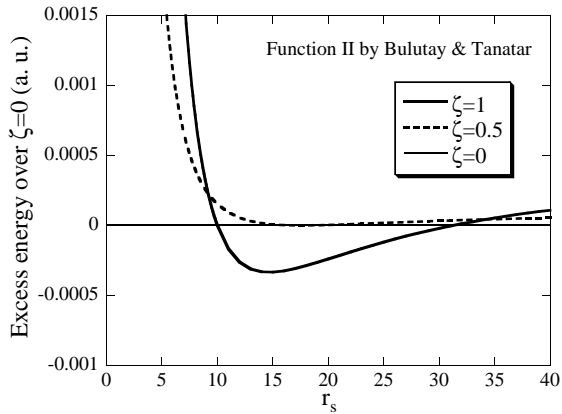


FIG. 5: Energy difference between polarizations by numerical simulation with mapping function II.

the same. Our simulation closely reproduces the polarization of the ground state of quantum simulations by Rapisarda and Senatore[6]. Since the differences of the energy between different polarization are very small especially in the case of mapping function II, it is difficult to say the range of r_s precisely where the ground state is polarized.

Numerical simulations based on the CHNC method are much easier to perform compared with first principle quantum simulations. The accuracy of results is not very high but may be enough to provide us with useful information on finite systems like quantum dots or the systems at finite temperatures. Simulations on some finite systems and bi-layer systems are now going on and will be reported elsewhere.

TABLE II: Helmholtz free energy in a.u. by numerical simulations with two different mapping functions. Italic means the lowest energy state in the same r_s values.

r_s	Mapping function I.			Mapping function II.		
	$\zeta = 0$	$\zeta = 0.5$	$\zeta = 1$	$\zeta = 0$	$\zeta = 0.5$	$\zeta = 1$
5	-0.14156	-0.13849	-0.13687	-0.15010	-0.14817	-0.14385
10	-0.08097	-0.08038	<i>-0.08169</i>	-0.08408	-0.08392	<i>-0.08408</i>
15	-0.05721	-0.05698	<i>-0.05798</i>	-0.05879	-0.05879	<i>-0.05913</i>
20	-0.04449	-0.04435	<i>-0.04503</i>	-0.04540	-0.04540	<i>-0.04564</i>
25	-0.03654	-0.03642	<i>-0.03687</i>	-0.03708	-0.03706	<i>-0.03720</i>
30	-0.03107	-0.03097	<i>-0.03125</i>	-0.03140	-0.03136	<i>-0.03142</i>
40	-0.02403	-0.02394	-0.02401	<i>-0.02412</i>	-0.02406	-0.02401

TABLE III: Helmholtz free energy in references. Italics mean the energy of $\zeta = 1$ is lower than that of $\zeta = 0$.

r_s	DMC[6]		DMC[7]		DMC[8]	
	$\zeta = 0$	$\zeta = 1$	$\zeta = 0$	$\zeta = 1$	$\zeta = 0$	$\zeta = 1$
5	-0.1490	-0.1433	-0.1498	-0.1429	-0.14952	-0.14361
10	-0.08512	-0.08448	-0.08545	-0.08404	-0.08543	-0.08458
20	-0.04620	-0.04620	-0.04634	-0.04612	-0.04628	-0.04625
30	-0.03187	<i>-0.03192</i>	-0.03196	-0.03190	-0.03194	-0.03194
40	-0.02439	<i>-0.02442</i>		-0.02442		

REFERENCES

- [1] M. W. C. Dharma-wardana and F. Perrot, Phys. Rev. Lett. **84**, 959 (2000).
- [2] F. Perrot and M. W. C. Dharma-wardana, Phys. Rev. Lett. **87**, 206404 (2001).
- [3] C. Bulutay and B. Tanatar, Phys. Rev. B **65**, 195116 (2002).
- [4] N. Q. Khan and H. Totsuji, Solid State Commun. **129**, 37 (2003).
- [5] N. Q. Khan and H. Totsuji, Phys. Rev. B **69**, 165110 (2004).
- [6] F. Rapisarda and G. Senatore, Aust. J. Phys. **49**, 161 (1996).
- [7] B. Tanatar and D. M. Ceperley, Phys. Rev. B **39**, 5005 (1989).
- [8] C. Attaccalite, S. Moroni, P. Gori-Giorgi, and G. B. Bachelet, Phys. Rev. Lett. **88**, 256601 (2002).